

Universal constrained power flow control for grid-tied power electronics converters

Citation for published version (APA):

González Duguet, C., Costa, L. F., & Papafotiou, G. (2025). Universal constrained power flow control for grid-tied power electronics converters. In *2025 European Control Conference, ECC 2025* (pp. 2557-2562). Article 11186873 Institute of Electrical and Electronics Engineers.
<https://doi.org/10.23919/ECC65951.2025.11186873>

Document license:
Unspecified

DOI:
[10.23919/ECC65951.2025.11186873](https://doi.org/10.23919/ECC65951.2025.11186873)

Document status and date:
Published: 14/10/2025

Document Version:
Accepted manuscript including changes made at the peer-review stage

Please check the document version of this publication:

- A submitted manuscript is the version of the article upon submission and before peer-review. There can be important differences between the submitted version and the official published version of record. People interested in the research are advised to contact the author for the final version of the publication, or visit the DOI to the publisher's website.
- The final author version and the galley proof are versions of the publication after peer review.
- The final published version features the final layout of the paper including the volume, issue and page numbers.

[Link to publication](#)

General rights

Copyright and moral rights for the publications made accessible in the public portal are retained by the authors and/or other copyright owners and it is a condition of accessing publications that users recognise and abide by the legal requirements associated with these rights.

- Users may download and print one copy of any publication from the public portal for the purpose of private study or research.
- You may not further distribute the material or use it for any profit-making activity or commercial gain
- You may freely distribute the URL identifying the publication in the public portal.

If the publication is distributed under the terms of Article 25fa of the Dutch Copyright Act, indicated by the "Taverne" license above, please follow below link for the End User Agreement:

www.tue.nl/taverne

Take down policy

If you believe that this document breaches copyright please contact us at:

openaccess@tue.nl

providing details and we will investigate your claim.

Universal constrained power flow control for grid-tied power electronics converters

Cristóbal González¹, Levy Costa¹, George Papafotiou¹

Abstract—With the increasing amount of energy resources connected to the electric powered grid via power electronics converters, commonly referred to as inverted-based resources (IBR), the inertia and robustness of power systems have been greatly impacted. Grid-forming control arose as a solution to these issues by operating the IBRs as voltage sources. However, limiting the amplitude of the converter current became an issue. In this context, the concept of a constrained control strategy capable of limiting the amplitude of the system variables gained relevance. As a solution, this work proposes a nonlinear model predictive control strategy, that is categorized neither as grid-forming nor grid-following. It is capable of controlling the power flow through the converter to the grid, without a phase-locked-loop, allowing constraint satisfaction even in the condition of unknown grid impedance. The control strategy was tested through simulation of nominal operation and during symmetric and asymmetric faults. The results proved its effectiveness in achieving these objectives even in cases in which the grid behavior cannot be predicted.

I. INTRODUCTION

Making the energy system greener has been a global task for the last several decades, and the integration of renewable resources through power converters is the key to it. A wide variety of inverter-based resources (IBR) are now integrated into power systems, adding controllability and flexibility to the system but negatively impacting some of its crucial aspects. As the share of power injected into the system by IBRs increases and the share of synchronous generators decreases, the overall inertia, inherently present in synchronous machines, is reduced. Therefore, the strength of the system is heavily affected. Additionally, in most cases, IBRs are operated by grid-following (GFL) controllers, meaning that the converter operates as current-controlled voltage sources by following and synchronizing with the grid voltage at the point of connection. This means that a mechanism to identify the voltage angular position is needed, which is mostly achieved by phase-locked loops (PLL). PLLs can work properly in strong grids; however, in weak grids, such as those with a high integration of IBR, their behavior is considerably disturbed by fluctuations in power flow at the point of connection to the grid, even leading to unstable system operation [1].

As a possible solution to these stability issues, grid-forming (GFM) is emerging as the enabling technology for

high penetration of IBRs [2]. Its main concept is to aim for the converter to behave as a voltage source that adjusts its voltage phasor (amplitude and phase) depending on the power being transferred to the grid. As synchronization between the converter and the grid is achieved through direct control of the power flow, many GFM controllers do not require a PLL to operate and have an auto-synchronizing feature, improving the stability and dynamic behavior of the system [3]. For the same reason, GFM converters have better fault-ride-through (FRT) performance than GFL converters.

However, because GFM converters do not directly control the converter current, large currents can be reached during faults. This might lead to the disconnection of IBRs to prevent the converter from being damaged, as they have limited overcurrent capability. This issue significantly affects the availability of power systems, as faults can easily lead to a shortage of services.

To prevent this from happening, many current limitation techniques have been proposed in recent years, with virtual impedance and reference saturation being among the most popular ones [4]. The former emulates a higher impedance at the output of the converter, whereas the latter saturates the references at different stages of the control loop (usually in the inner current control loop) to keep them below a certain amplitude. Although these strategies can provide current limitation, they generally present instability issues and trouble recovering from the fault condition [4]. Additionally, there is no direct constraint on the current of the converter, which can also result in transient overcurrents [5]. To deal with stability issues during faults, a new current-limitation cross-forming control was developed [6], controlling the amplitude of the converter current by leaving its voltage amplitude to be driven by the system, which can become a problem because of overvoltages [7].

All these examples illustrate the relevance of designing a strategy that can naturally limit the amplitude of a state of the system by directly posing constraints [8], not only on currents but also on voltages at different points in the system. Such a strategy would ensure the safe operation of the converter and the system. In this line, this work proposes a nonlinear model predictive control (NMPC) approach, as MPC is known for its natural capability of dealing with constraints and nonlinear systems. To prevent stability issues caused by PLLs, this strategy avoids them by directly modeling the system through the power flow equations, resulting in a nonlinear system. Notice that this implies that any linear control strategy used to directly control power (such as traditional GFM control) must be

*This project is supported and financed by Alfen N.V. and co-financed by Holland High Tech with PPP-allowance for research and development in the HTSM top sector

¹All authors are with the Electromechanics and Power Electronics group, Department of Electrical Engineering, Eindhoven University of Technology, Eindhoven, the Netherlands

{c.a.gonzalez.duguet,l.costa,g.papafotiou}@tue.nl

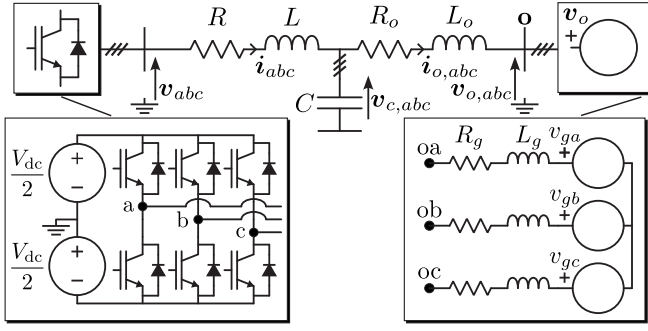


Fig. 1: Diagram of an LCL filter grid-tied voltage source converter.

based on a linearized model [9]. The proposed approach is inspired by the power flow control presented in [10]; however, this work aims for a single control loop that poses constraints directly on the states of the system and not on their references. Additionally, the proposed strategy relies on parameters that are nominally known to the designer and assumes the voltage at the point of connection as a disturbance, reducing the impact of uncertainties. Finally, the proposed strategy achieves a balanced-voltage-source-behind-impedance behavior, which is something that some grid codes demand nowadays [11].

II. MODEL OF THE SYSTEM

The connection of an IBR to a grid is commonly done through a filter, with LCL filters being the most common type. Consider the LCL-filter grid-tied voltage source converter (VSC) in Fig. 1, connected to a system with nominal frequency ω_n . All three-phase variables can be expressed in the quadrature dq rotating-frame system $\xi_{dq} = [\xi_d \xi_q]^\top$, where

$$\xi_{dq} = \frac{2}{3} \begin{bmatrix} \cos(\theta) & \cos\left(\theta - \frac{2\pi}{3}\right) & \cos\left(\theta + \frac{2\pi}{3}\right) \\ -\sin(\theta) & -\sin\left(\theta - \frac{2\pi}{3}\right) & -\sin\left(\theta + \frac{2\pi}{3}\right) \end{bmatrix} \xi_{abc}$$

with $\xi_{abc} = [\xi_a \xi_b \xi_c]^\top$ and θ being an arbitrary angular position, which is defined as

$$\theta(t) = \omega_n t + \theta_0 \quad (1)$$

where θ_0 is an arbitrary initial angular position. The grid to which the converter is connected is modeled as a Thevenin equivalent, which means that the parameters R_g and L_g , and the voltage $v_{g,abc}$ are only a representation of a more complex system and do not necessarily exist in reality, since they are only abstractions of the behavior of the real system. On the other hand, controlling the DC link voltage is outside the scope of the work, so it is assumed to be constant and perfectly stiff. A state-space representation of the system can be written as

$$\begin{aligned} \dot{\mathbf{x}}(t) &= \mathbf{F}\mathbf{x}(t) + \mathbf{G}\mathbf{u}(t) + \mathbf{M}\mathbf{w}(t), \\ \mathbf{y}(t) &= f(\mathbf{x}(t)), \end{aligned} \quad (2)$$

where the state, input and disturbance vectors are defined as $\mathbf{x} = [\mathbf{i}_{dq}^\top \mathbf{i}_{o,dq}^\top \mathbf{v}_{c,dq}^\top]^\top$, $\mathbf{u} = \mathbf{v}_{dq}$ and $\mathbf{w} = \mathbf{v}_{o,dq}$, with \mathbf{i}_{dq} the converter currents, $\mathbf{v}_{c,dq}$ the capacitor voltages, $\mathbf{i}_{o,dq}$ the grid currents, \mathbf{v}_{dq} the converter voltages, and $\mathbf{v}_{o,dq}$ the voltages at point \mathbf{o} . Here, voltages v_{abc} and $v_{o,abc}$ are defined with respect to the ground point depicted in Fig. 1. The dynamic equations of the system are derived from Kirchhoff's laws, with all variables and parameters in per unit [12]. The system matrices result in

$$\begin{aligned} \mathbf{F} &= \omega_B \begin{bmatrix} -\frac{R}{L}\mathbf{I}_2 - \omega_n \mathbf{J} & \mathbf{0}_2 & -\frac{1}{L}\mathbf{I}_2 \\ \mathbf{0}_2 & -\frac{R_o}{L_o}\mathbf{I}_2 - \omega_n \mathbf{J} & \frac{1}{L_o}\mathbf{I}_2 \\ \frac{1}{C}\mathbf{I}_2 & -\frac{1}{C}\mathbf{I}_2 & -\omega_n \mathbf{J} \end{bmatrix}, \\ \mathbf{G} &= \frac{\omega_B}{L} [\mathbf{I}_2 \ \mathbf{0}_{4 \times 2}]^\top, \quad \mathbf{M} = -\frac{\omega_B}{L_o} [\mathbf{0}_2 \ \mathbf{I}_2 \ \mathbf{0}_2]^\top, \end{aligned}$$

where \mathbf{I}_n is the identity matrix of order n , $\mathbf{0}_{n \times m}$ is an n by m zero matrix, $\mathbf{0}_n$ is a square zero matrix of order n , and

$$\mathbf{J} = \begin{bmatrix} 0 & -1 \\ 1 & 0 \end{bmatrix}.$$

Regarding the output of the system, the controller must regulate the power flow in the output of the converter and follow specific references. Therefore, the output $\mathbf{y}(k) = f(\mathbf{x}(k)) = [pq]^\top$, are the instantaneous active and reactive power p and q defined as

$$p = v_{cd}i_d + v_{cq}i_q, \quad q = v_{cq}i_d - v_{cd}i_q. \quad (3)$$

Most grid-following strategies rely on identifying the angle θ_0 of (1) to perfectly align the position of the reference frame with the grid voltage. Then, the expression of power at the point \mathbf{o} becomes linear. This is done by means of a PLL, which in the case of weak networks is prone to unstable behavior. To avoid relying on a PLL, the proposed approach does not seek to align the reference frame with the grid voltage and defines the power as in (3). Although it makes the system nonlinear, it prevents all the potential issues that arise from PLLs.

Model (2) can be discretized with a sampling period T_s using exact discretization, resulting in

$$\begin{aligned} \mathbf{x}(k+1) &= \mathbf{A}\mathbf{x}(k) + \mathbf{B}\mathbf{u}(k) + \mathbf{T}\mathbf{w}(k), \\ \mathbf{y}(k) &= f(\mathbf{x}(k)), \end{aligned} \quad (4)$$

where the matrices are $\mathbf{A} = e^{\mathbf{F}T_s}$, $\mathbf{B} = -\mathbf{F}^{-1}(\mathbf{I}_6 - \mathbf{A})\mathbf{G}$, and $\mathbf{T} = -\mathbf{F}^{-1}(\mathbf{I}_6 - \mathbf{A})\mathbf{M}$.

III. MODEL PREDICTIVE CONTROL PROBLEM

The system is controlled by solving an optimization problem, in real time, at each instant k , every T_s seconds. The states of the system are sampled at each time step, with $\mathbf{x}(k) = \mathbf{x}_0$ being the sampled states and $\mathbf{w}(k) = \mathbf{w}_0$ the sampled disturbance. The MPC problem considers a prediction horizon of N steps, and employs a receding horizon policy. The strategy's main objective is to always provide a balanced-voltage-source-behind-impedance behavior (i.e., $v_{c,abc}$ have to be balanced and change as slowly as possible, which is equivalent to $v_{c,dq}$ being as constant as possible). During balanced conditions (normal operation), it

should properly track active and reactive power references. These objectives should be met while limiting the converter's current and the filter capacitor voltage to be within specified limits.

A. Cost function

The cost function of the MPC problem must consider all the objectives, therefore the following is proposed

$$J = J_y + J_v + J_u \quad (5)$$

comprising the three terms

$$J_y = \sum_{\ell=k+1}^{k+N} \|\mathbf{y}^*(\ell) - \mathbf{y}(\ell)\|_{\lambda^y}^2, \quad (6a)$$

$$J_v = \lambda^v \sum_{\ell=k+1}^{k+N} \|\delta_{vc}(\ell)\|^2, \quad (6b)$$

$$J_u = \lambda^u \sum_{\ell=k}^{k+N-1} \|\delta_u(\ell)\|^2, \quad (6c)$$

where \mathbf{y}^* is the vector of references for \mathbf{y} , $\delta_{vc}(\ell) = \mathbf{v}_{c,dq}(\ell) - \mathbf{v}_{c,dq}(\ell-1)$ and $\delta_u(\ell) = \mathbf{v}_{dq}(\ell) - \mathbf{v}_{dq}(\ell-1)$, whereas

$$\lambda^y = \begin{bmatrix} \lambda^p & 0 \\ 0 & \lambda^q \end{bmatrix},$$

and the \mathbf{K} – weighted norm is defined as

$$\|\xi\|_{\mathbf{K}} := \sqrt{\xi^T \mathbf{K} \xi} \quad (7)$$

with \mathbf{K} being a positive definite matrix. On the other hand, λ^p , λ^q , λ^v , and λ^u are weighting factors, tuned to define the priorities among the objectives. The term J_y in the cost function penalizes both active and reactive power tracking errors, addressing the first control objective. On the other hand, J_v penalizes the rate of change of $\mathbf{v}_{c,dq}$, for it to be as constant as possible, so the variables in the abc frame are as balanced as possible, therefore leading to a balanced internal voltage behind impedance in steady state. Lastly, the term J_u is added to penalize large changes in control decisions along the prediction horizon, regulating the aggressiveness and speed of the control loop.

B. Constraints

One of the main contributions of the proposed controller lies in the direct bounding applied to the system states, enhancing the safety of the converter and system. Limiting the variables is achieved by defining appropriate constraints in the optimization problem, as shown below.

1) *Converter voltage constraint:* The output voltages that a VSC can generate are defined by the topology used. For a two-level converter, the feasible voltage that the converter can apply in each phase is bounded by $\pm V_{dc}/2$, which results in a cubical box constraint in the static reference frame abc . In the rotating dq frame, that box is equivalent to a rotating hexagon, as depicted in Fig.2. In this work, motivated by implementation simplicity, the hexagon is approximated by its inscribed circle of radius $V_{dc}/\sqrt{3}$ shown in Fig.2. All

the box constraints detailed below were approximated in the same manner. Hence, the converter voltage is constrained as

$$\mathbf{v}_{dq}^T \mathbf{v}_{dq} \leq \left(\frac{V_{dc}}{\sqrt{3}} \right)^2. \quad (8)$$

2) *Converter current limitation:* Power electronics devices have limited overcurrent and overvoltage capabilities [7]. Therefore, large currents, such as those during faults, can cause damage to the converter or the activation of protection mechanisms that would disconnect the converter and curtail the service provided. Hence, it is relevant to ensure that the converter currents are smaller than the maximum value they can conduct. This is expressed as

$$\mathbf{i}_{dq}^T \mathbf{i}_{dq} \leq I_{\max}^2. \quad (9)$$

3) *Capacitor voltage constraint:* Grid codes generally define a voltage range considered as normal operation, usually for the range 0.9 – 1.1 p.u. [11]. Furthermore, since overvoltages can damage the converter [7] and increase the capacitor failure over time, limiting the voltage of the filter capacitor is desirable. Therefore, to protect the converter and the filter from overvoltages, the following constraint is added

$$\mathbf{v}_{c,dq}^T \mathbf{v}_{c,dq} \leq V_{\max}^2. \quad (10)$$

C. MPC problem formulation

The resulting MPC problem that is solved at each control instant k is

$$\min_{\mathbf{u}(\ell), \forall \ell \in \mathcal{K}_{0:N-1}} \sum_{\ell=k+1}^{k+N} \|\mathbf{y}^*(\ell) - \mathbf{y}(\ell)\|_{\lambda^y}^2 + \sum_{\ell=k+1}^{k+N} \|\delta_{vc}(\ell)\|_{\lambda^v}^2 + \sum_{\ell=k}^{k+N-1} \|\delta_u(\ell)\|_{\lambda^u}^2 \quad (11a)$$

s.t.

$$\mathbf{x}(\ell+1) = \mathbf{A}\mathbf{x}(\ell) + \mathbf{B}\mathbf{u}(\ell) + \mathbf{T}\mathbf{w}(\ell), \quad \forall \ell \in \mathcal{K}_{0:N-1} \quad (11b)$$

$$\mathbf{y}(\ell) = f(\mathbf{x}(\ell)), \quad \forall \ell \in \mathcal{K}_{1:N} \quad (11c)$$

$$\mathbf{x}(k) = \mathbf{x}_0 \quad (11d)$$

$$\mathbf{w}(\ell) = \hat{\mathbf{w}}(\ell), \quad \forall \ell \in \mathcal{K}_{0:N-1} \quad (11e)$$

$$\mathbf{i}_{dq}^T(\ell) \mathbf{i}_{dq}(\ell) \leq I_{\max}^2, \quad \forall \ell \in \mathcal{K}_{1:N} \quad (11f)$$

$$\mathbf{v}_{c,dq}^T(\ell) \mathbf{v}_{c,dq}(\ell) \leq V_{\max}^2, \quad \forall \ell \in \mathcal{K}_{1:N} \quad (11g)$$

$$\mathbf{v}_{dq}^T(\ell) \mathbf{v}_{dq}(\ell) \leq \left(\frac{V_{dc}}{\sqrt{3}} \right)^2, \quad \forall \ell \in \mathcal{K}_{0:N-1} \quad (11h)$$

where (11b) and (11c) are the system's state–space equations, used for the prediction of the states and outputs along the prediction horizon, (11d) is the measurement of the states, used as an initial condition to the prediction, (11e) introduces the estimation $\hat{\mathbf{w}}$ of the disturbance along the prediction horizon, (11f) and (11g) are the limitation of the system states, and (11h) is the feasible set of the actuation. To define the prediction horizon, the set $\mathcal{K}_{\eta:\xi} = \{k + \eta, \dots, k + \xi\}$, comprising consecutive instants starting from $k + \eta$, with $\eta < \xi$, is used.

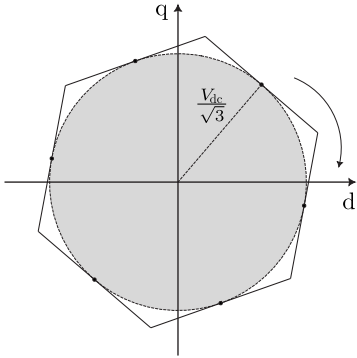


Fig. 2: Feasible set (hexagon) of a two-level VSC and its approximation (inscribed circle).

Two things must be mentioned regarding (11). First, the cost function is non-convex, therefore, proving the optimality of the solution is not trivial. On the other hand, in a real setup, the strategy will be implemented by formulating (11f) and (11g) as soft constraints, to avoid eventual infeasible instances. However, the analysis of persistent feasibility considering the hard-constrained formulation would yield a more rigorous analysis of the characteristics of the problem and will be the subject of future work.

IV. SIMULATION RESULTS

The proposed strategy was tested through simulation of the system in Fig.1 using the parameters in Table I. The optimization problem was solved using *acados* [13], an open source software package comprising solvers for non-linear optimal control, designed to be fast in embedded control platforms. The solver was initialized with the previous solution. Given the relatively slow dynamics of the system compared to the sampling time, this is a valid starting point. A prediction horizon of $N = 50$ was used, as the objective of this work is to explore the best possible performance. The sampling frequency was set at 10 kHz, and the modulation strategy used was symmetric space vector modulation (SVM). The strategy was tested in three different scenarios: an active power step, a symmetric voltage dip (three-phase fault), and an asymmetric voltage dip (2-phase fault). There are no external control loops, as the scope is to analyze the behavior of the MPC strategy itself. However, external power control loops can be incorporated. In all cases, the reactive power reference is adjusted according to the active power reference, so the capacitor voltage is approximately 1 pu when the grid voltage is also 1 pu, and no reactive power is transferred to the grid. The weighting factors were set to prioritize balanced voltage at the filter capacitor, aiming for the converter and the filter to behave as a balanced voltage source behind impedance from the grid's perspective. During faults, emergency weighting factors are allowed to modify the priorities of control objectives, as will be explained for each case.

Two conditions were evaluated in each scenario: the first is the ideal case, in which there is complete information about the system, that is, disturbances can be perfectly

TABLE I: System parameters for simulation

Parameter	Value	Parameter	Value
S_{nom}	20 kVA	V_g	$220\sqrt{2}$ V (L-N)
I_{nom}	42.9 A (RMS)	V_{dc}	800 V
R	0.138 pu	R_o	0.0344 pu
L	0.1082 pu	L_o	0.0865 pu
R_g	0.0344 pu	C	0.2281 pu
L_g	0.1731 pu		

predicted (meaning that $v_{o,dq}$ is perfectly known, so $\hat{w}(k) = w(k), \forall k$), and thus emergency weights can be applied instantly. In the realistic case, disturbances are assumed to be constant throughout the prediction horizon and equal to the measured disturbance w_0 at instant k (i.e., $\hat{w}(\ell) = w_0, \forall \ell \in \mathcal{K}_{0:N-1}$), although $v_{o,dq}$ can actually change over time. This assumption leads to errors in the predicted behavior whenever the system is not in a perfectly balanced steady state (constant $v_{o,dq}$); however, the controller is expected to perform correctly despite those prediction errors. Additionally, in this case, the emergency weights are applied only 10 ms after the fault occurred, to emulate a more realistic operation where the detection of a fault is not instantaneous.

During normal operation, for the ideal case, in which the disturbance is perfectly predicted, the weighting factors were set as $\lambda^p = \lambda^q = 1$, and $\lambda^v = \lambda^u = 10$. In the realistic case, where large prediction errors can exist, a less aggressive and slower controller is needed to reduce the effect of the disturbances. Therefore, the weighting factors in this case were set as $\lambda^p = \lambda^q = 1$, and $\lambda^v = \lambda^u = 100$. For every case and scenario, the active and reactive power, current and voltage limiting constraints, and the capacitor voltages in the dq reference frame are plotted to verify all control objectives.

A. Active power step

The system is initialized with zero power transferred by the converter to the grid. A 1 pu step in p^* is applied (simultaneously with a small q^* step to keep the voltage amplitude constant). The results for the ideal case are shown in Fig. 3. Notice how both active and reactive power references are quickly tracked even though the capacitor voltage limit is reached during the transient. It is worth noting that all constraints are perfectly respected, and the steady state is reached quickly without significant oscillations in the capacitor voltage. It is important to note that there is a steady state error in the tracking of q^* , caused by the harmonics introduced by the SVM, which are not considered in the system model. Given that these harmonics can be considerably reduced by simply increasing the switching frequency of the semiconductors, this issue is not analyzed in this work. In Fig. 4, the results for the realistic case are presented. During normal operation, the grid voltage $v_{g,dq}$ is constant and the voltage at the point of connection $v_{o,dq}$ suffers only small transients. Therefore, the prediction errors are small. As a result, even though there is an uncertain weak grid, the performance is almost identical to the ideal case, and all constraints are met.

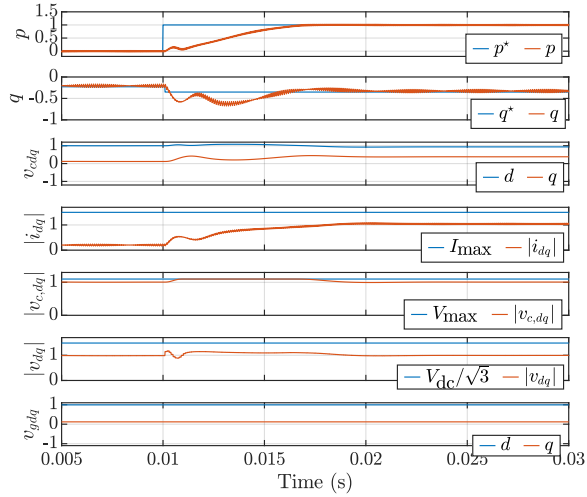


Fig. 3: Traces during p^* step for ideal case.

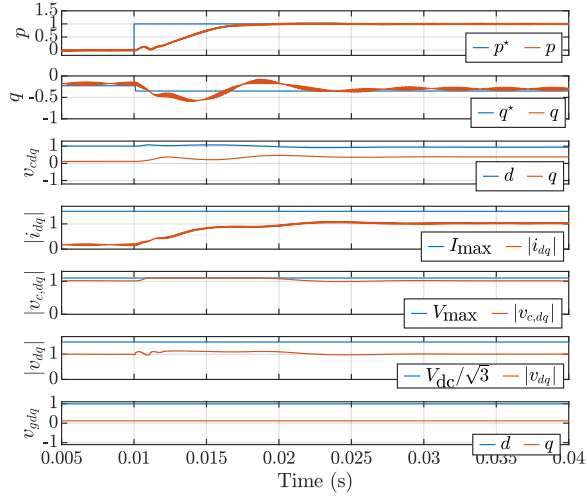


Fig. 4: Traces during p^* step for realistic case.

B. Symmetric voltage dip

With the converter operating at nominal active power, a symmetric voltage dip of 0.1 pu is applied to $v_{g,abc}$. During the dip, the tracking of the reactive power is removed from the objectives in both the ideal and realistic cases by setting $\lambda^q = 0$.

In the ideal case, the emergency weighting factors λ^p and λ^v remain unchanged, while $\lambda^u = 100$ is set to avoid aggressive responses. In contrast, in the realistic case, $\lambda^p = 10^{-4}$, λ^u remains constant and $\lambda^v = 10^4$ is applied to prevent excessive oscillations and achieve balanced capacitor voltages. The results for each respective case are shown in figures 5 and 6.

The expected performance of the converter during a 3-phase fault is to inject its maximum allowed current as quickly as possible, helping the protection system identify the fault, without following the active and reactive power references. In the ideal case, this objective is achieved quickly and straightforwardly, with the current limit reached within a few milliseconds while complying with all constraints. In

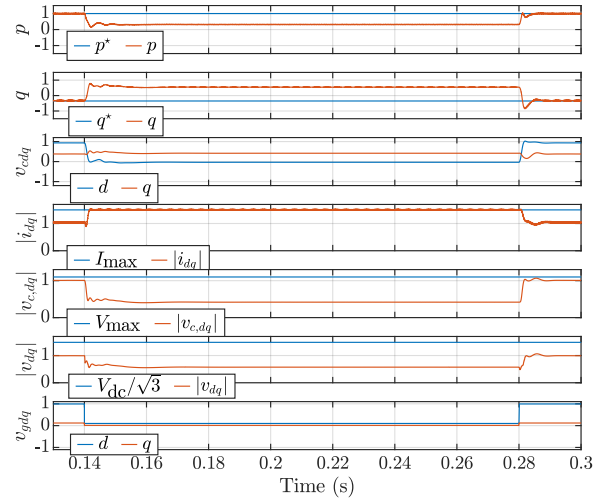


Fig. 5: Traces during a 3-phase symmetric dip for ideal case.

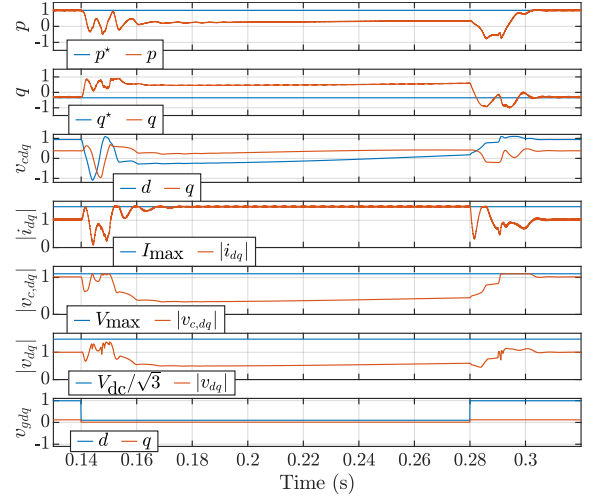


Fig. 6: Traces during a 3-phase symmetric dip for realistic case.

the realistic case, the converter withstands the fault without violating any constraints. As soon as the emergency weights are applied, the converter behaves as desired. Notice that the normal steady state is recovered once the weighting factors return to normal, after the fault is cleared.

C. Asymmetric voltage dip

With the system in nominal operation, two phases of $v_{g,abc}$ drop to 0.4 pu, while the third remains at 1 pu. This results in a highly unbalanced $v_{g,abc}$, leading to a significant presence of negative sequence. Since the negative sequence induces oscillations in the system states, a high priority must be given to balancing the capacitors to reduce the effect of negative sequence. During the fault, $\lambda^q = 0$ in both cases. In the ideal case, the emergency weights are set to $\lambda^p = 10^{-3}$, λ^u remains constant, and $\lambda^v = 10^5$.

In the realistic case, due to the negative sequence, errors in the system predictions become significant. Consequently, $\lambda^p = 10^{-5}$, λ^u remain unchanged, and $\lambda^v = 10^4$ is applied

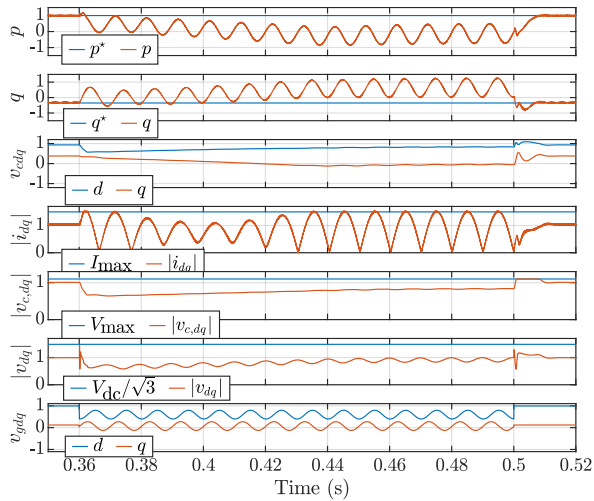


Fig. 7: Traces during a 2-phase dip for ideal case.

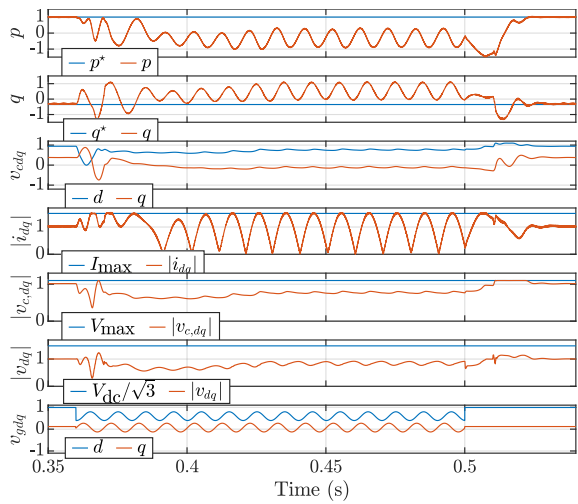


Fig. 8: Traces during a 2-phase dip for realistic case.

to balance capacitor voltages despite the large uncertainties and oscillations in $v_{o,dq}$. The traces for this case are shown in figures 7 and 8.

In the ideal case, the voltages of the capacitors exhibit very small oscillations and the changes are smooth. Naturally, by forcing the capacitor voltages to remain balanced, both the active and reactive powers exhibit significant oscillations. In the realistic case, immediately after the emergency weights are applied, the behavior becomes as desired, with the oscillations in the capacitor voltages reduced while complying with constraints. Note that the current limit is reached in both cases, which is the primary reason the voltages are not perfectly balanced.

V. CONCLUSION AND FUTURE WORK

This work presents a nonlinear MPC strategy for grid-tied power electronics converters, capable of controlling the power flow between the converter and the grid without the need for a PLL. In addition, it can directly constrain the predicted system states to ensure safe operation.

The strategy was tested through simulation, and its performance was analyzed by comparing an ideal case, where disturbances are perfectly known, with a case where the grid behavior is uncertain. The results showed not only proper tracking of active and reactive power references during normal operation but also that the system states never violate amplitude limits, not even during symmetrical or asymmetrical faults.

The real-time deployment of the strategy in commercial control hardware is the next research step. In practical applications such an algorithm would need to be executed in the range of tens to a few hundreds of microseconds. For such timescales, the execution times reported in the literature with tools such as `acados` appear to be sufficient. However, guaranteeing maximum execution times and persistent feasibility under these conditions presents us with a research challenge that will require both theoretical treatment and careful consideration of practical characteristics, and the approximations that these might allow.

REFERENCES

- [1] Y. Wu, H. Wu, F. Zhao, Z. Li, and X. Wang, "Influence of pll on stability of interconnected grid-forming and grid-following converters," *IEEE Transactions on Power Electronics*, vol. 39, no. 10, pp. 11 980–11 985, Oct 2024.
- [2] J. Matevosyan, B. Badrzadeh, T. Prevost, E. Quitmann, D. Ramasubramanian, H. Urdal, S. Achilles, J. MacDowell, S. H. Huang, V. Vital, J. O'Sullivan, and R. Quint, "Grid-forming inverters: Are they the key for high renewable penetration?" *IEEE Power and Energy Magazine*, vol. 17, no. 6, pp. 89–98, Nov 2019.
- [3] R. Rosso, X. Wang, M. Liserre, X. Lu, and S. Engelken, "Grid-forming converters: Control approaches, grid-synchronization, and future trends—a review," *IEEE Open Journal of Industry Applications*, vol. 2, pp. 93–109, 2021.
- [4] N. Baeckeland, D. Chatterjee, M. Lu, B. Johnson, and G.-S. Seo, "Overcurrent limiting in grid-forming inverters: A comprehensive review and discussion," *IEEE Transactions on Power Electronics*, vol. 39, no. 11, pp. 14 493–14 517, Nov 2024.
- [5] B. Fan, T. Liu, F. Zhao, H. Wu, and X. Wang, "A review of current-limiting control of grid-forming inverters under symmetrical disturbances," *IEEE Open Journal of Power Electronics*, vol. 3, pp. 955–969, 2022.
- [6] X. He, M. A. Desai, L. Huang, and F. Dörfler, "Cross-forming control and fault current limiting for grid-forming inverters," 2024. [Online]. Available: <https://arxiv.org/abs/2404.13376>
- [7] T. Guillod, F. Krismer, and J. W. Kolar, "Protection of mv converters in the grid: The case of mv/lv solid-state transformers," *IEEE Journal of Emerging and Selected Topics in Power Electronics*, vol. 5, no. 1, pp. 393–408, March 2017.
- [8] D. Groß and X. Lyu, "Towards constrained grid-forming control," in *2023 59th Annual Allerton Conference on Communication, Control, and Computing (Allerton)*, Sep. 2023, pp. 1–6.
- [9] L. Zhang, L. Harnefors, and H.-P. Nee, "Power-synchronization control of grid-connected voltage-source converters," *IEEE Transactions on Power Systems*, vol. 25, no. 2, pp. 809–820, 2010.
- [10] G. Beccuti, G. Papafotiou, and L. Harnefors, "Multivariable optimal control of hvdc transmission links with network parameter estimation for weak grids," *IEEE Transactions on Control Systems Technology*, vol. 22, no. 2, pp. 676–689, March 2014.
- [11] National Energy System Operator, "The complete grid code. Issue 6, Revision 27, 01 October 2024. [Online] Available: <https://dcm.nationalenergyso.com/> (Revisited: October 7th, 2024)."
- [12] T. Geyer, *Model Predictive Control of High Power Converters and Industrial Drives*. Wiley, 2016.
- [13] R. Verschueren, G. Frison, D. Kouzoupis, J. Frey, N. van Duijkeren, A. Zanelli, B. Novoselnik, T. Albin, R. Quirynen, and M. Diehl, "acados – a modular open-source framework for fast embedded optimal control," *Mathematical Programming Computation*, 2021.